



Synthesis, Characterization and Dyeing Performance of Co(II), Ni(II), Cu(II) and Zn(II) Complexes with (E)-4-Chloro-N-(2-(Dimethylamino)Ethyl)-5-((8-Hydroxyquinolin-5-yl)Diazenyl)-2-Methoxybenzamide

Hanna Hashim Mohammed¹  and Amer J. Jarad^{2*} 

^{1,2}Department of Chemistry, College of Education for Pure Science (Ibn Al-Haitham), University of Baghdad
Baghdad, Iraq.

*Corresponding author

Received: 22/May/2025

Accepted: 2/September/2025

Published: 20/ January /2026

doi.org/10.30526/39.1.4205



© 2026. The Author(s). Published by College of Education for Pure Science (Ibn Al-Haitham), University of Baghdad. This is an open-access article distributed under the terms of the [Creative Commons Attribution 4.0 International License](https://creativecommons.org/licenses/by/4.0/)

Abstract

The (E)-4-chloro-N-(2-(dimethylamino)ethyl)-5-((8-hydroxyquinolin-5-yl)diazenyl)-2-methoxybenzamide azo ligand (L) has been synthesized through the reaction of diazonium salt for 5-amino-4-chloro-N-(2-(dimethylamino) ethyl)-2-methoxybenzamide with 8-hydroxyquinoline and identified azo ligand (L) using spectroscopic studies (FTIR, UV-Vis, ¹H and ¹³CNMR, mass), and micro-elemental analysis (C.H.N). Metal chelates of Co(II), Ni(II), Cu(II), as well as Zn(II) have been completed as well as characterized using mass spectra, flame atomic absorption, elemental analysis (C.H.N), infrared, UV-Vis spectroscopy, as well as conductivity, magnetic measurements. The metal-to-ligand ratio in all complexes, as determined by analytical data, was 1:2 and exhibited a tetrahedral structure of the prepared complexes with the ligand, as the ligand is linked to the metal ions through the N atom of the (C=N) group and the substituted OH-group, which has lost its proton to form a stable five-membered ring with the 8-hydroxyquinoline compound. Then, colors play a significant role in detergent stability and brightness during the dyeing of composite materials produced on cotton fabrics. Therefore, solid dyes exhibit excellent color stability and depth of texture.

Keywords: 5-Amino-4-chloro-N-(2-(dimethylamino)ethyl)-2-methoxybenz-amide, Azo dyes, Dyeing performance, Textile industry.

1. Introduction

Azo dyes are a significant class of dyes utilized in a wide range of technological and scientific applications, accounting for over half of all dyes and commercial colors^{1,2}. Research has also focused on azo dyes containing heterocyclic rings due to their distinct properties³. The use of heterocyclic rings as coupling components has enabled the development of dyes with strong chromophores, vivid colors, and high levels of dyeing and fastness properties⁴. Azo compounds are becoming increasingly important in the future as they are considered among the most productive dyes (more than 60%)⁵. Disperse dyes are renowned for their luster, colorfastness, and durability, as well as their economic and environmental benefits when used in dyeing polyester fabrics^{6,7}. A surfactant is used to disperse water-dispersed dyes, which are limited in solubility, before they are applied to polyester fabrics^{8,9}. Metal azo complexes have made significant contributions to the development of drugs, particularly anticancer drugs. These complexes represent novel, low-cost compounds with a broad range of antimicrobial, anti-inflammatory, and anticancer activities^{10,11}. The organic compound 8-hydroxyquinoline is of great importance in applications due to its ability to bind various metal ions, serving as a disubstituted ligand^{12,13}. The current study aims to design and synthesize azo compounds, along with Co(II), Ni(II), Cu(II), and Zn(II) compounds from (E)-4-chloro-N-(2-(dimethylamino)

ethyl)-5-((8-hydroxyquinolin-5-yl)diazenyl)-2-methoxybenzamide. These compounds are characterized using various physicochemical methods. No doubt, the applied sciences have significant industrial applications.

2. Materials and Methods

2.1. Instrumentation

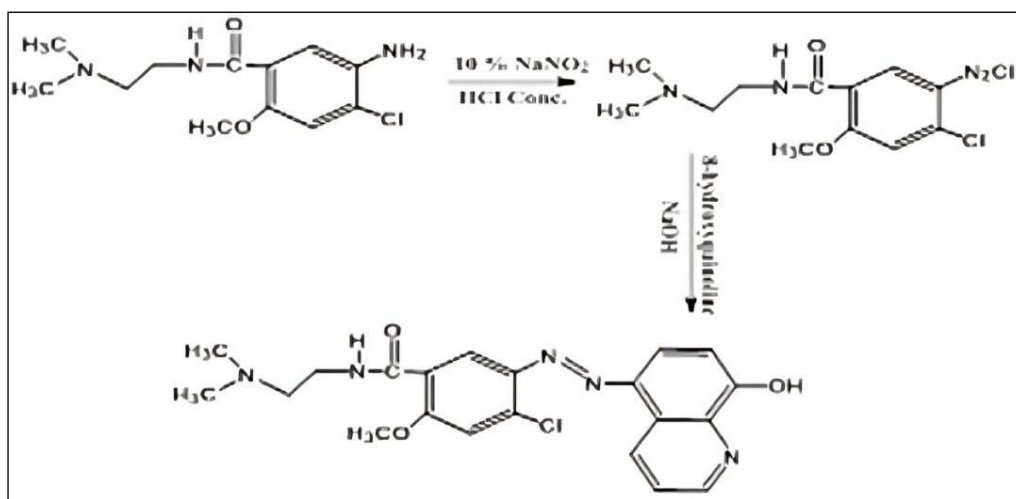
At the University of Basra in Iraq, ^{13}C and ^1H NMR spectra were obtained on a Bruker 400 MHz UltraShield spectrometer. Dimethyl sulfoxide (DMSO) was used as the solvent, while tetramethylsilane was used as the reference. The conductivity of the prepared compounds dissolved in ethyl alcohol at a concentration of 10^{-3} M was measured at 25 degrees Celsius with a Philips PW-Digital Conductance meter. For micro elemental analysis (C.H.N), an Eurovector EA 3000, version 3.0, has been appointed. Scientists enhanced the magnetic properties using Sherwood's Auto Magnetic Susceptibility measurement at 25 degrees Celsius. Atomic absorbance was assessed with a Shimadzu A.A-160 A Atomic Absorption/ Flame Emission Spectrophotometer. The UV-visible spectrum was recorded using a UV-Vis-160A spectrophotometer. Infrared spectra of the samples were recorded as KBr disks and analyzed using a Shimadzu FTIR-8400S Fourier Transform Infrared Spectrophotometer over the range of $4000\text{-}400\text{ cm}^{-1}$. Mass spectrometry measurements were taken using a Shimadzu (E170 EV) Spectrometer, and melting points were determined employing a Stuart Melting Point Apparatus.

2.2. Materials and reagents

All for chemicals $\text{CoCl}_2 \cdot 6\text{H}_2\text{O}$, $\text{NiCl}_2 \cdot 6\text{H}_2\text{O}$, $\text{CuCl}_2 \cdot 2\text{H}_2\text{O}$ also ZnCl_2 have been supplied from B.D.H, while 5-amino-4-chloro-N-(2-(dimethylamino)ethyl)-2-methoxybenzamide also 8-hydroxyquinoline obtained from Merck.

2.3. Preparation of the ligand

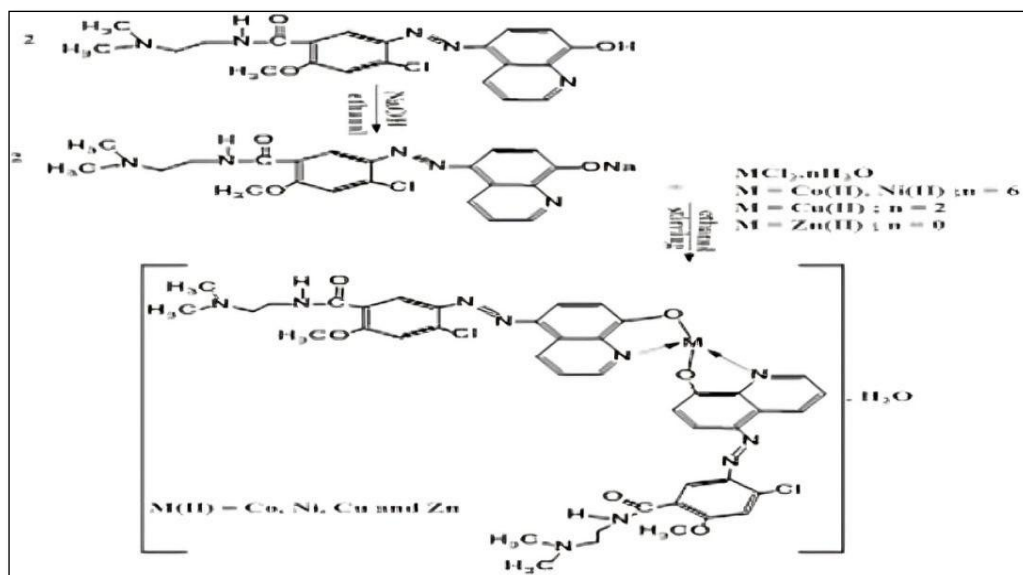
The 5-amino-4-chloro-N-(2-(dimethylamino) ethyl)-2-methoxybenzamide¹⁴ (0.678 g, 1 mmol), which was dissolved in a mixture consisting of (10 mL $\text{C}_2\text{H}_5\text{OH}$, 2 mL conc. HCl), was also denitrified at 5°C utilizing a 10% solution of NaNO_2 . After adding the diazotized collyrium solution, the mixture was stirred in a cold ethanolic solution (0.362 g, 1 mmol) of 8-hydroxyquinoline. After that, 25 mL of a solution (1M NaOH) has been added to the dark-coloured mixture, and the formation of the azo compound is noticed through its precipitation. After filtering the sediment, it is washed with a large volume of (1:1) $\text{C}_2\text{H}_5\text{OH}:\text{H}_2\text{O}$, after which the sediment is left to dry. The reaction is shown in **Scheme 1**.



Scheme 1. Preparation steps for azo ligand (L)

2.4. Preparation for metal chelates

EtOH solution from ligand (0.854 g, 2 mmole) containing (0.08 g, 2 mmol NaOH), added a drop of the wisdom of stirring, to 0.237, 0.237, 0.170, also 0.136 g from $\text{CoCl}_2 \cdot 6\text{H}_2\text{O}$, $\text{NiCl}_2 \cdot 6\text{H}_2\text{O}$, $\text{CuCl}_2 \cdot 2\text{H}_2\text{O}$, also ZnCl_2 , resolved on aqueous solution (pH=7). The mixture is cooled until the precipitate turns dark, then filtered and washed with several ounces of a 1:1 $\text{H}_2\text{O} : \text{C}_2\text{H}_5\text{OH}$ mixture. **Scheme 2** shows the preparation technique, along with its physical features, C.H.N. The analysis is presented in **Table 1**.



Scheme 2. Proposed structure from metal (II) compounds of azo ligand (L)

Table 1. Physical features into azo ligand also metal chelates

Compounds	Color	M.P°C	Yield%	Analysis Calc (Found)			
				M%	C%	H%	N%
Ligand(L)	Deep brown	220-222	87	-	58.94 (57.93)	5.14 (4.91)	16.37 (15.92)
$[\text{Co}(\text{L})_2] \cdot \text{H}_2\text{O}$	Brown	300-302	82	6.34 (6.13)	54.19 (53.93)	4.73 (4.07)	15.05 (14.88)
$[\text{Ni}(\text{L})_2] \cdot \text{H}_2\text{O}$	Reddish brown	>360	80	6.24 (6.03)	54.25 (53.45)	4.73 (4.09)	14.06 (14.91)
$[\text{Cu}(\text{L})_2] \cdot \text{H}_2\text{O}$	Pal brown	320-322	85	6.84 (5.93)	53.90 (52.95)	4.70 (4.12)	14.97 (13.85)
$[\text{Zn}(\text{L})_2] \cdot \text{H}_2\text{O}$	Brown	280-282	81	6.94 (5.68)	53.84 (52.91)	4.70 (4.03)	14.95 (13.92)

2.5. Dyeing process

Chemicals are applied to cotton fibers, which are available in dyeing grades that provide a 1% shade variation. The fabric dyeing process takes 1 hour at temperatures between 15 and 20 °C, with a pH of 10.

3. Results

The association of the azo ligand (L) with 5-amino-4-chloro-N-(2-(dimethylamino)ethyl)-2-methoxybenzamide for diazotization is suitable for alkaline conditions in terms of performance. Spectroscopic studies and elemental analysis were performed on the prepared ligand. Solid complexes were produced by reacting a ligand dissolved in ethanol with metal ions dissolved in a buffer solution (pH= 7) at a ratio of (metal: ligand) = 1:2. The experimental results from both elemental analysis and metal content measurements closely matched the calculated theoretical

values. The conductivity of ligands, as well as of metal chelates dissolved in ethanol (10^{-3} mol/L), is of the non-electrical type¹⁵, as shown in **Table 2**.

3.1. NMR spectra

Figures 1 and 2 show the ^1H , ^{13}C NMR spectra of the ligand (L), which display multiple chemical shifts.

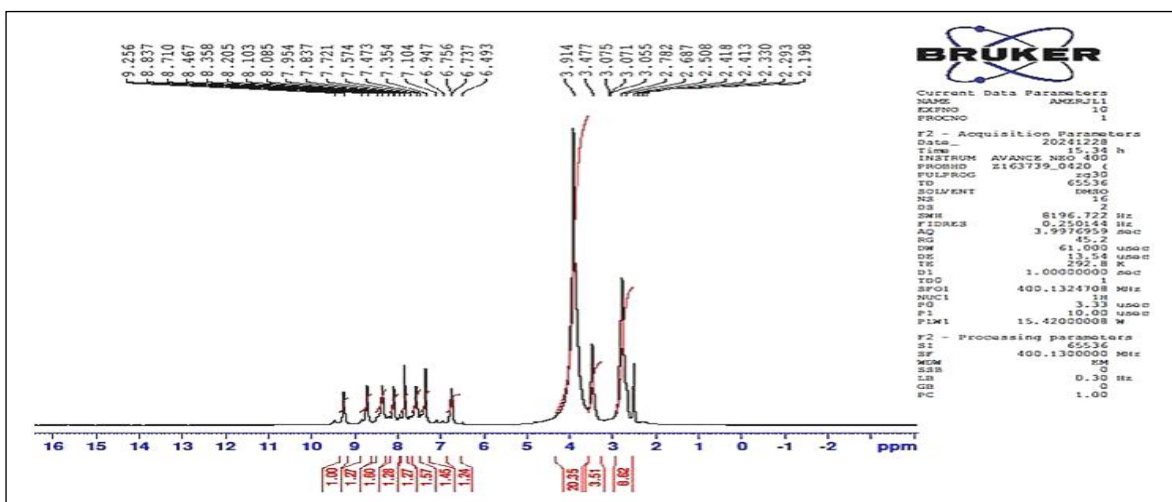


Figure 1. The ^1H NMR spectrum for azo ligand (L)

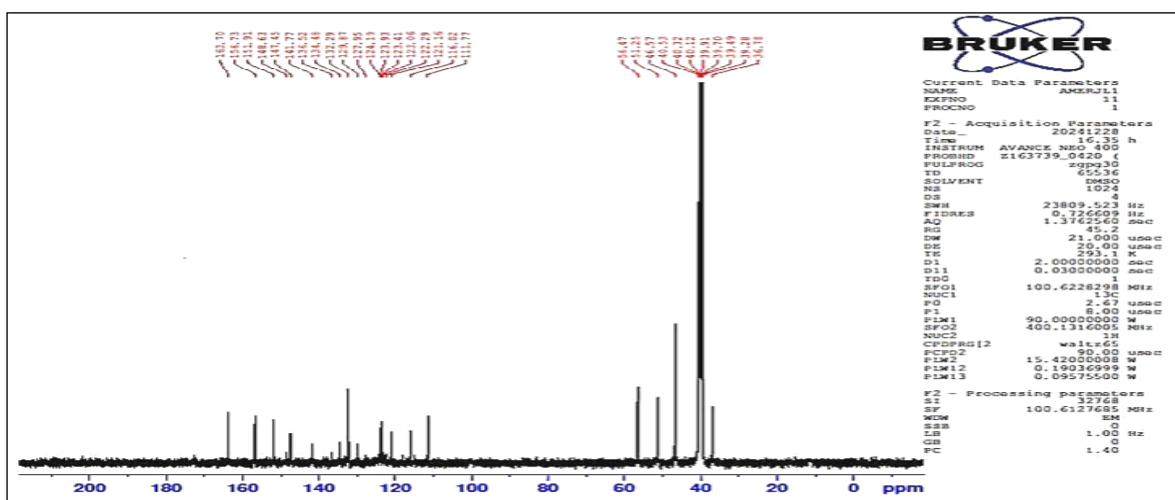
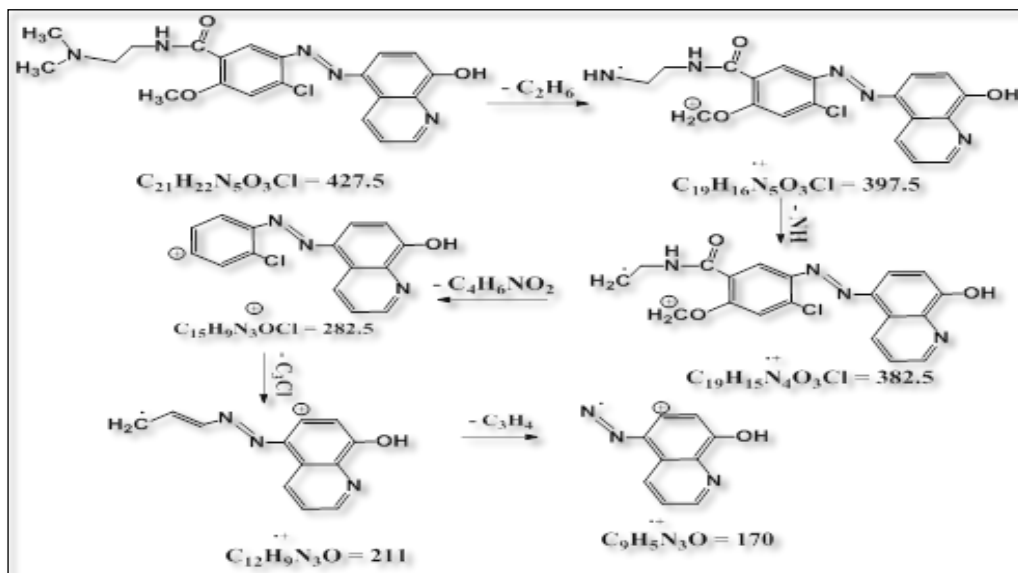


Figure 2. The ^{13}C NMR spectrum for azo ligand (L)

3.2. Mass spectra

From the mass spectrometric analysis of the azo ligand (L), the peak was observed at $m/z = 427.5$, which is also due to the formula $\text{C}_{21}\text{H}_{22}\text{N}_5\text{O}_3\text{Cl}$. For a summary of the general pattern of segmentation according to **Scheme 3** and **Figure 3**. The complexes appeared in mass spectra as peaks centered at $m/z = 912$, 911 , 917 , and 918 , corresponding to the formulas $[\text{C}_{42}\text{H}_{42}\text{N}_{10}\text{O}_6\text{Cl}_2\text{Co}]$, $[\text{C}_{42}\text{H}_{42}\text{N}_{10}\text{O}_6\text{Cl}_2\text{Ni}]$, $[\text{C}_{42}\text{H}_{42}\text{N}_{10}\text{O}_6\text{Cl}_2\text{Cu}]$, and $[\text{C}_{42}\text{H}_{42}\text{N}_{10}\text{O}_6\text{Cl}_2\text{Zn}]$, respectively. Based on the general segmentation pattern, the summary is based on **Schemes 4-7** and **Figures 4-7**.



Scheme 3. Retail style for azo ligand (L)

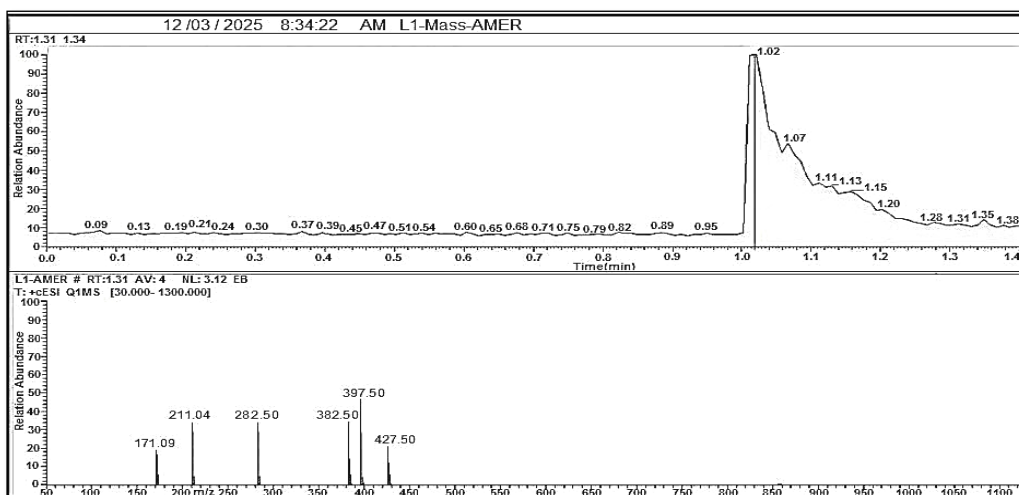


Figure 3. Mass spectrum for azo ligand (L)

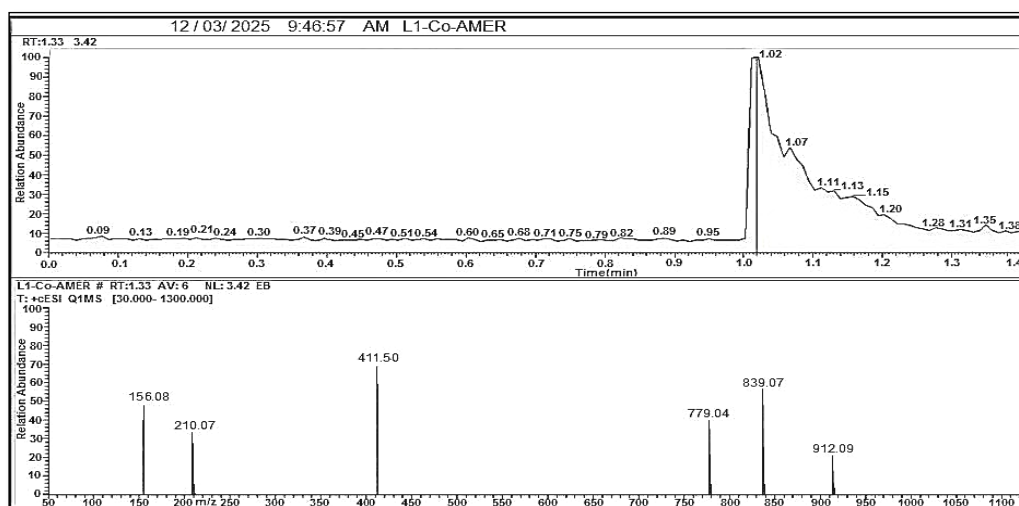


Figure 4. Mass spectrum for [Co(L)₂].H₂O complex

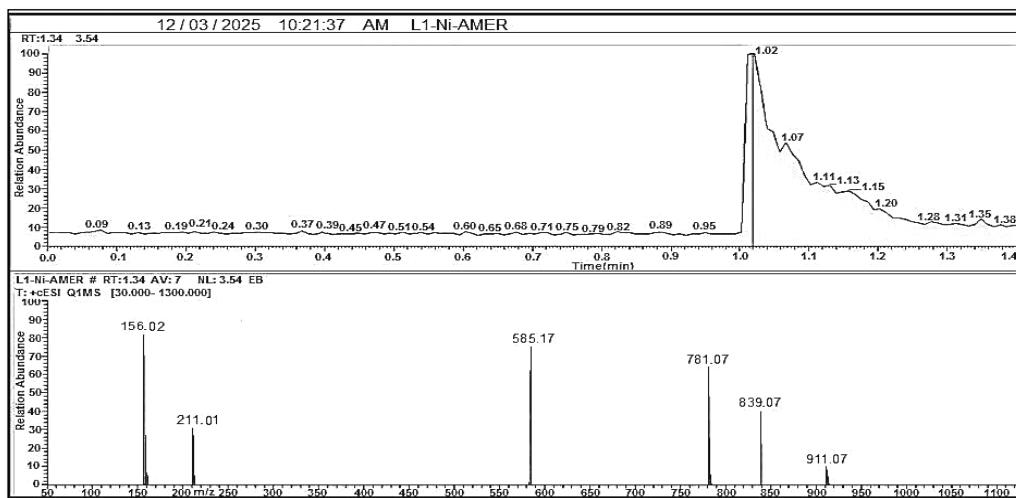


Figure 5. Mass spectrum for $[\text{Ni}(\text{L})_2]\cdot\text{H}_2\text{O}$ complex

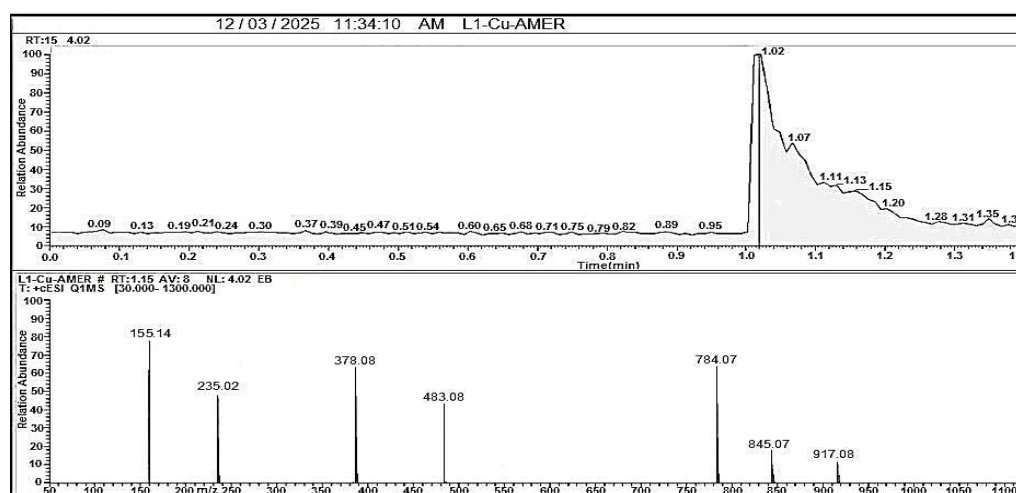


Figure 6. Mass spectrum for $[\text{Cu}(\text{L})_2]\cdot\text{H}_2\text{O}$ complex

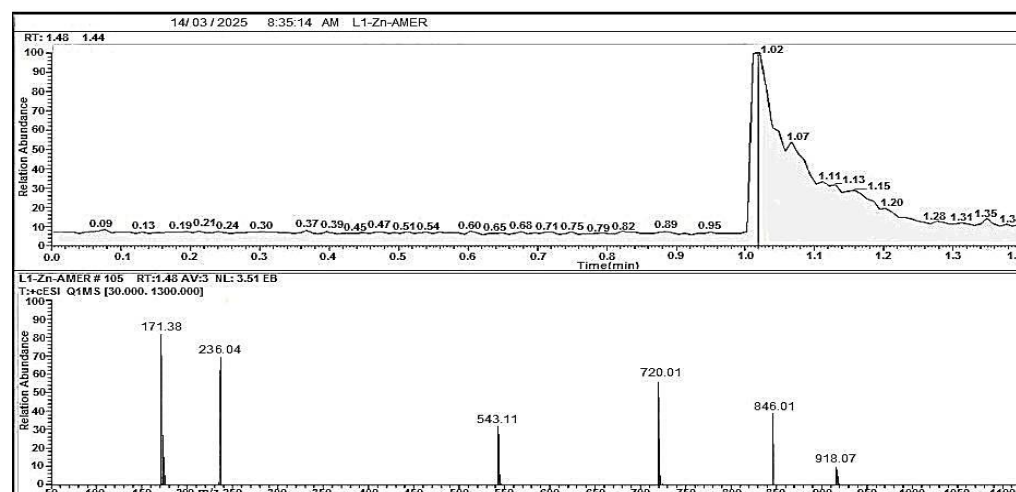
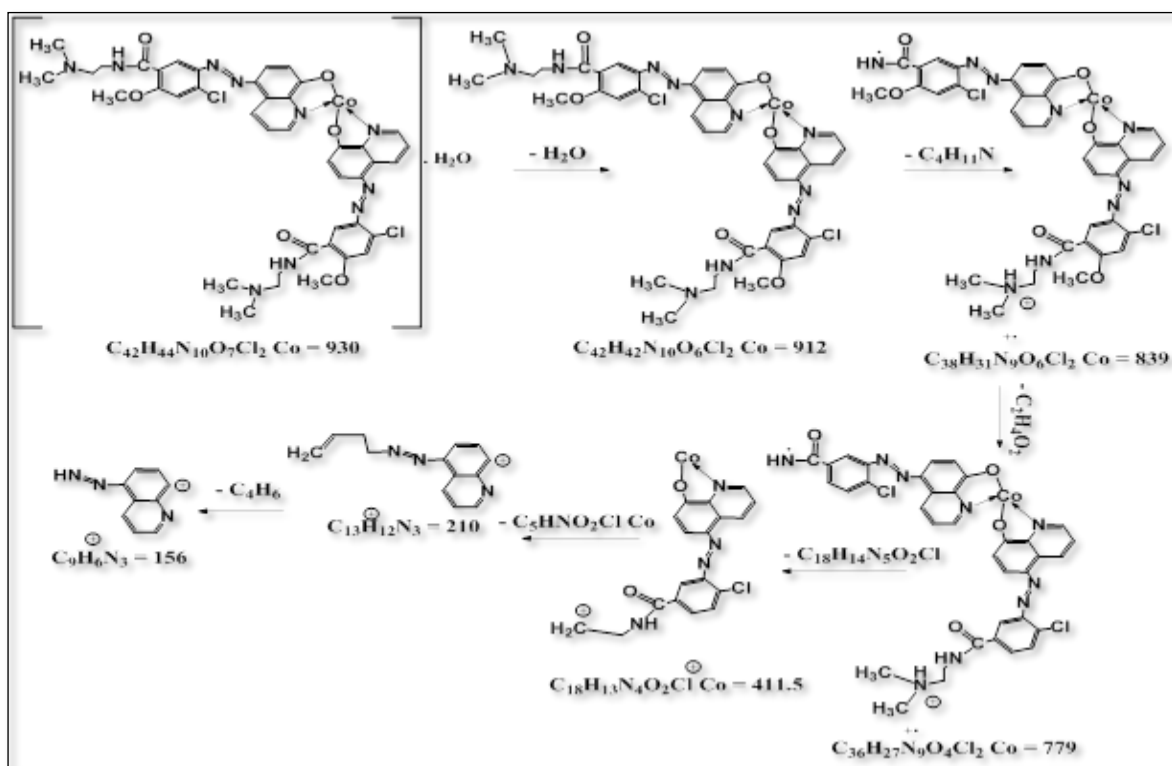
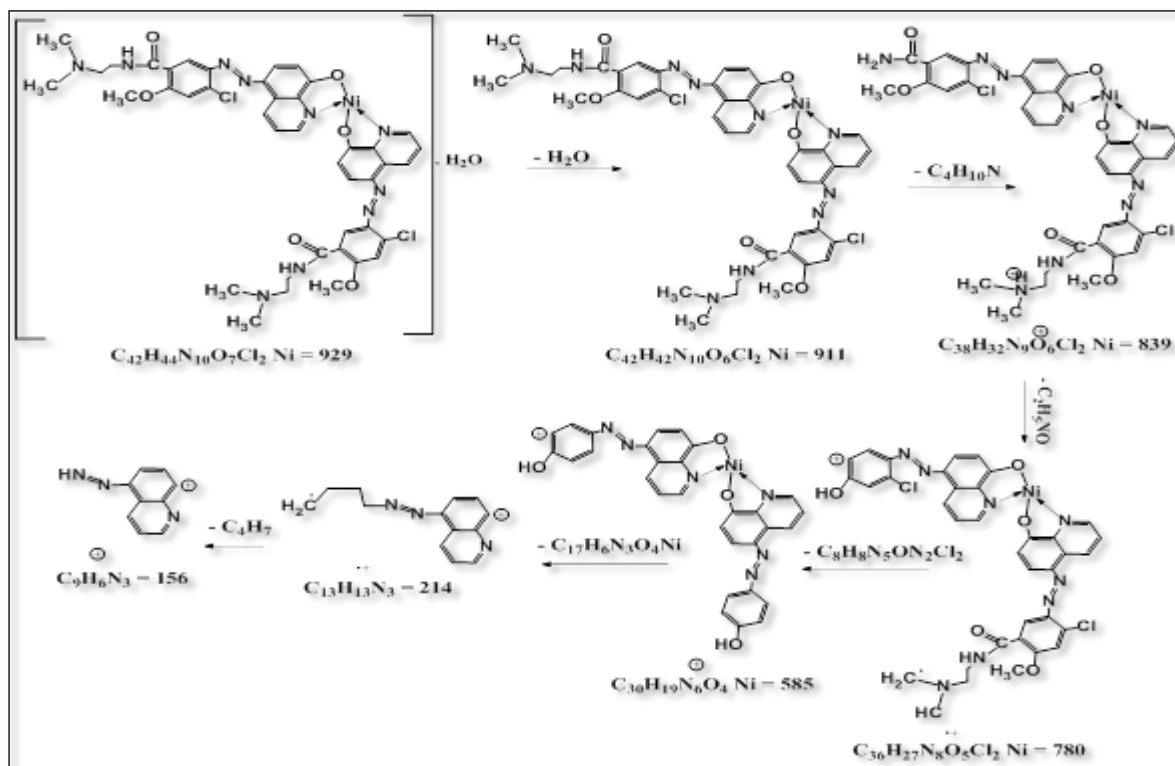


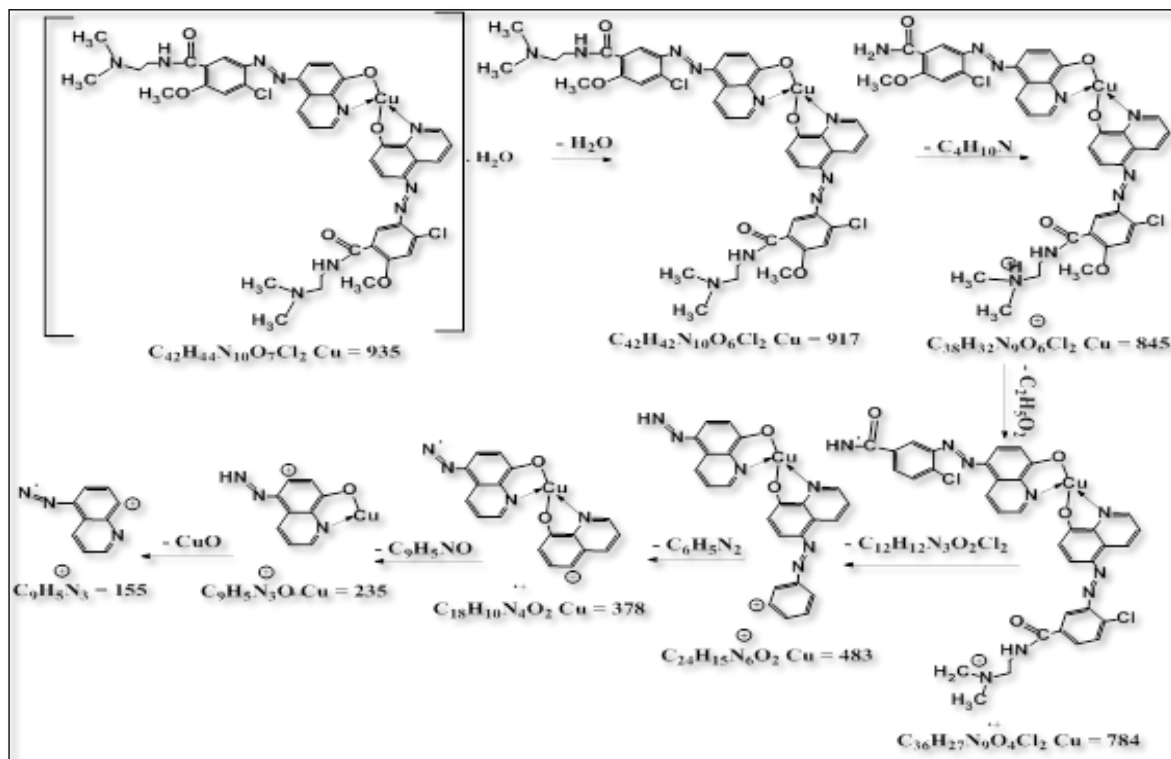
Figure 7. Mass spectrum for $[\text{Zn}(\text{L})_2]\cdot\text{H}_2\text{O}$ complex



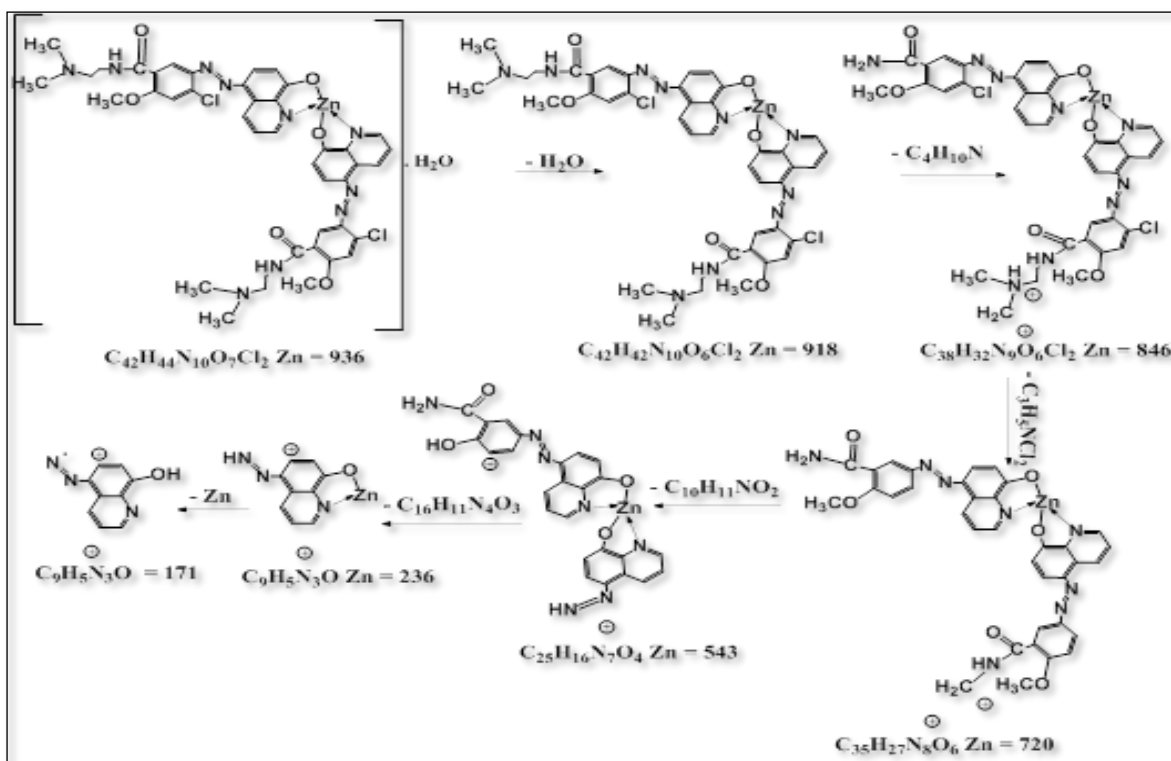
Scheme 4. Retail style for $[Co(L)_2].H_2O$ complex



Scheme 5. Retail style for $[Ni(L)_2].H_2O$ complex



Scheme 6. Retail style for $[Cu(L)_2].H_2O$ complex



Scheme 7. Retail style for $[Zn(L)_2].H_2O$ complex

3.3. Electronic spectra

The UV-Vis spectra of the prepared complexes, resolved in ethyl alcohol (10^{-3} mol/L), were measured, along with the compositional data listed in **Table 2**.

Table 2. Electronic spectrum data with compounds, magnetic properties as well molar conductivity on ethanol (1×10^{-3} M)

Compounds	λ nm	ν cm^{-1}	ABS	ϵ $\text{L.mol}^{-1}\text{cm}^{-1}$	Assignment	Λ $\text{S.cm}^2 \text{mol}^{-1}$	μ_{eff} B.M
Ligand(L)	244 430	40983 23255	1.510 1.200	1510 1200	$\pi-\pi^*$ $n-\pi^*$	-	-
[Co(L) ₂].H ₂ O	250 487 757 861 982	40000 20533 13210 11614 10183	0.700 0.780 0.005 0.006 0.036	700 780 5 6 36	Intra ligand C.T $^4A_{2(F)} \rightarrow ^4T_{1(P)}$ $^4A_{2(F)} \rightarrow ^4T_{1(F)}$ $^4A_{2(F)} \rightarrow ^4T_{2(F)}$	7.82	4.68
[Ni(L) ₂].H ₂ O	260 319 507 732 852 888	38461 31347 19723 13661 11737 11261	0.850 0.360 1.210 0.007 0.007 0.051	850 360 1210 7 7 51	Intra ligand Intra ligand C.T $^3T_{1(F)} \rightarrow ^3T_{1(P)}$ $^3T_{1(F)} \rightarrow ^3A_{2(F)}$ $^3T_{1(F)} \rightarrow ^3T_{2(F)}$	5.65	3.90
[Cu(L) ₂].H ₂ O	258 327 469 962	38759 30581 21321 10395	1.290 0.580 0.940 0.007	1290 580 940 7	Intra ligand Intra ligand C.T $^2T_2 \rightarrow ^2E$	6.05	2.07
[Zn(L) ₂].H ₂ O	245 453	40816 22075	1.280 0.840	1280 840	Intra ligand C.T	9.35	Dia

3.4. FTIR spectra

From summing the FTIR spectrum of the azo (L) bond, as well as metal chelates, with the tabulation of the data in **Table 3**.

Table 3. Infrared spectroscopic information of azo ligand (L) also its metal chelates (cm^{-1})

Compounds	$\nu(\text{OH})+\nu(\text{H}_2\text{O})$	$\nu(\text{C=O})+\nu(\text{C=N})$	$\nu(\text{C=C})+\nu(\text{N=N})$	$\nu(\text{M-N})+\nu(\text{M-O})$
Ligand(L)	3350 br. -	1633 sh. 1591 sh.	1560 s. 1544 s. 1467 sh.	-
[Co(L) ₂].H ₂ O	- 3356 br.	1639 sh. 1575 s.	1552 sho. 1544 sho. 1462 sh.	536 w. 468 w.
[Ni(L) ₂].H ₂ O	- 3400 br.	1635 s. 1575 sh.	1552 s. 1545 sho. 1467 sh.	536 w. 470 w.
[Cu(L) ₂].H ₂ O	- 3385 br.	1633 sh. 1581 sh.	1556 sho. 1544 s. 1467 sh.	491 w. 445 w.
[Zn(L) ₂].H ₂ O	- 3408 br.	1633 sh. 1573 sh.	1556 s. 1544 sho. 1469 sh.	532 w. 472 w.

r = broad, sh = sharp, s = strong, w = weak, sho =shoulder.

3.5. Dyeing performance

The finished chemicals that dye cotton fabrics have already been determined. The brightness and stability of a cleaner depend on its colors. Therefore, solid dyes exhibit excellent color stability and texture depth. The coloring is illustrated in **Figure 8**.

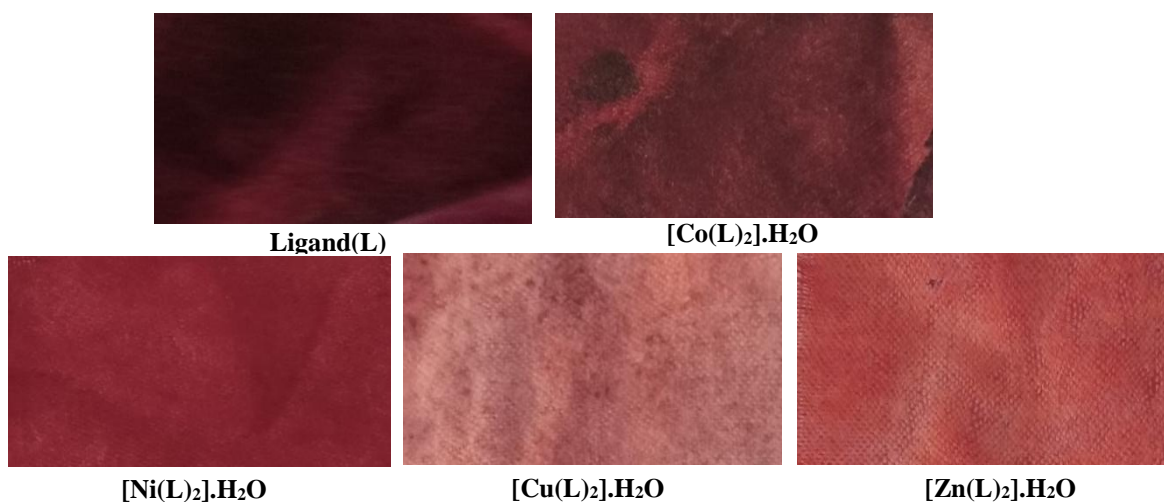


Figure 8. Textile dyeing utilizing azo ligand also metal chelates

4. Discussion

4.1. NMR spectra

The ^1H NMR spectrum at ligand (L), which shows multiple chemical shifts in the range ($\delta=6.493\text{-}8.467$ ppm) due to the protons of the benzene ring¹⁶. The spectrum also showed shifts on ($\delta=9.256$ ppm as well as ($\delta=8.710$ ppm) because the protons at hydroxyl and amine groups, respectively¹⁷. The shifts at ($\delta=2.687, 3.075$ ppm as well ($\delta=2.293$ ppm) are due to $\delta(2\text{CH}_2)$ as well $\delta(2\text{CH}_3)$, as well as the shifts at ($\delta=3.477$ ppm), ($\delta=2.50$ ppm) also ($\delta=3.914$ ppm) are because $\delta(\text{OCH}_3)$, DMSO- d_6 and DHO, respectively¹⁸. The ^{13}C NMR spectrum for ligand (L) showed signals on $\delta=46.57$ ppm as well $\delta=51.25$ ppm because the carbons of the methyl groups $\delta(\text{CH}_3)$ and $\delta(\text{OCH}_3)$ respectively. Signals on ($\delta=36.78$ ppm as well as ($\delta=56.47$ ppm) are due to the carbon of the ethylene group $\delta(\text{CH}_2\text{CH}_2)$. The spectrum also showed shifts in the range ($\delta=147.45\text{-}111.77$ ppm) due to the carbon at aromatic rings, while the shifts on ($\delta=163.70, 156.73, 151.91, 148.63$ ppm) are because the carbon on carbonyl group (C=O), methoxy (C-OCH₃), hydroxyl (C-OH), and (C=N), respectively. The shift at ($\delta=40.12$ ppm) is due to DMSO- d_6 ^{19,20}.

4.2. Electronic spectra

Intense absorption peaks of the azo ligand from the spectrum width at 244 and 430 nm, which were assigned to the electronic transition ($\pi\text{-}\pi^*$) as well as ($n\text{-}\pi^*$)²¹. Co^{II} spectrum appears two peaks on 250 as well 487 nm back to intra ligand also charge transfer, peaks at 757, 861 also 982 nm which were specified unto electronic transition type $^4\text{A}_{2(\text{F})}\rightarrow^4\text{T}_{1(\text{P})}$, $^4\text{A}_{2(\text{F})}\rightarrow^4\text{T}_{1(\text{F})}$ as well as $^4\text{A}_{2(\text{F})}\rightarrow^4\text{T}_{2(\text{F})}$ respectively, also magnetic moment value at 4.68 B.M this would be further evidence from tetrahedral geometry²². The Ni^{II} complex exhibited peaks at 260, 319, and 507 nm, which were attributed to intra-ligand and charge-transfer transitions. Other peaks at 732, 852, and 888 nm lead to electronic transition type $^3\text{T}_{1(\text{F})}\rightarrow^3\text{T}_{1(\text{P})}$, $^3\text{T}_{1(\text{F})}\rightarrow^3\text{A}_{2(\text{F})}$ as well as $^3\text{T}_{1(\text{F})}\rightarrow^3\text{T}_{2(\text{F})}$. The magnetic moment at the compound was found to be 3.90 B.M that was closer unto tetrahedral environment²³. The spectrum of the Cu^{II} complex showed peaks at 258, 327, and 469 nm attributed to intra-ligand and charge transfer. Peak on 962 nm, which has been assigned $^2\text{T}_2\rightarrow^2\text{E}$, The magnetic moment for the complex was 2.07 BM, which is closest to that of a tetrahedral environment²⁴. The electronic spectrum of the Zn^{II} complex shows charge-transfer bands, and the magnetic susceptibility indicates that the complex is a diamagnetic, because d-d transitions are not possible; hence the electronic spectrum did not yield fruitful information. In fact, this result is in agreement with previous work on tetrahedral geometry²⁵.

4.3. FTIR spectra

The ligand spectrum showed an absorption band at 3350 cm^{-1} because of the vibrational frequency of the $\nu(\text{OH})$ group. Disappearance of this group in the spectra of the prepared complexes is clear evidence of the occurrence of coordination with the metal ion²⁶. The ligand also showed a sharp and high-intensity band at 1633 cm^{-1} , which is due to the stretching

frequency of the $\nu(\text{C}=\text{O})$ group. This band did not exhibit any noticeable change in the spectra of the prepared complexes, indicating that it does not participate in the coordination process with the metal ion²⁷. The band at 1591 cm^{-1} in the ligand spectrum is due to the vibrations of the $\nu(\text{C}=\text{N})$ group. This band has undergone numerous changes in position and intensity within the complex spectra, in addition to occasional splitting or the appearance of shoulder bands beside it as it shifted towards a lower frequency, which is believed to be one of the coordination sites with the metal ion²⁸. The spectrum of the ligand showed bands at 1544 , 1560 cm^{-1} , and 1467 cm^{-1} , which are attributed to the $\nu(\text{C}=\text{C})$ group and the bridging azo group $\nu(\text{N}=\text{N})$, respectively. These bands did not show any noticeable changes in the spectra of the prepared complexes, indicating that they do not coordinate to the metal ion²⁹. All compounds exhibited new bands in the region $(445\text{-}536)\text{ cm}^{-1}$, which are due to the $\nu(\text{M}-\text{O})$ as well as $\nu(\text{M}-\text{N})$ bond vibrations. Their appearance is attributed to coordination between the metal and the nitrogen in the group $(\text{C}=\text{N})$, as well as the oxygen in the phenol group after losing a proton to the 8-hydroxyquinoline^{30,31}. The prepared complexes also exhibited new bands in the region $(3356\text{-}3408)\text{ cm}^{-1}$, which are attributed to the stretching frequency of hydrate water³².

5. Conclusion

To summarize, this study involved using an azo ligand to form coordination complexes with Co, Ni, Cu, and Zn ions. Various methods, including melting point determination, conductivity measurements, magnetic properties, and spectroscopic analysis (^{13}C and ^1H NMR, UV-Vis, FTIR, and mass spectrometry), were employed to characterize the ligand and its complexes. The analytical and spectroscopic results indicated the tetrahedral shape of the prepared complexes with the ligand, as the ligand is linked to the metal ions through the N atom of the $(\text{C}=\text{N})$ group and the substituted OH- group, which has lost its proton to form a stable five-membered ring with the 8-hydroxyquinoline compound. The dyeing abilities were tested, revealing that both the ligand and its complexes demonstrated vigorous activity.

Acknowledgment

The authors thank the Department of Chemistry, College of Education for Pure Sciences (Ibn Al-Haitham), University of Baghdad, for their support in providing the essential materials needed to carry out this research successfully.

Conflict of Interest

The authors declare that they have no conflicts of interest.

References

1. Mohsin AK, Ali HM. Analytical studies of new azo dye and the diminished in their biological activity by complexation with Zinc. *Bio Chem Sci.* 2025; 4(3):88-96. <https://doi.org/10.5281/zenodo.16652335>.
2. Akram D, Elhaty IA, AlNeyadi SS. Synthesis and antibacterial activity of rhodanine based azo dyes and their use as spectrophotometric chemosensor for Fe^{3+} ions. *Chemosensors.* 2022; 8(1):16. <https://doi.org/10.3390/chemosensors8010016>.
3. Abouzayed FI, Abouel-Enein SA, Hammad AM. Synthesis of some novel nanosized chelates of anchoring bisazo dye 5-[5-(4,6-dioxo-2-thioxo-hexahydro-pyrimidin-5-ylazo)-naphthalen-1-ylazo]-2-mercapto-1h-pyrimidine-4,6-dione and their applications as antioxidant and antitumor agents. *ACS Omega.* 2021; 6(42):27737–27754. <https://doi.org/10.1021/acsomega.1c02989>.
4. Jasim DJ, Abbas AK. Synthesis, identification, antibacterial, medical and dyeing performance studies for azo-sulfamethoxazole metal complexes. *Eurasian Chem Comm.* 2022; 4(1):16–40. <https://doi.org/10.22034/ecc.2022.310593.1251>.

5. Cui MH, Liu WZ, Tang ZE, Cui D. Recent advancements in azo dye decolorization in bio-electrochemical systems (BESs): insights into decolorization mechanism and practical application. *Water Res.* 2021; 203:117512. <https://doi.org/10.1016/j.watres.2021.117512>.
6. Mohammadi A, Khalili B, Tahavor M. Novel push-pull heterocyclic azo dyes containing piperazine moiety: Synthesis, spectral properties, antioxidant activity and dyeing performance on polyester fibers. *Spectrochim. Acta Part A Mol Biomol Spectrosc.* 2015; 150:799–805. <https://doi.org/10.1016/j.saa.2015.06.024>.
7. Rahman MM, Haque TMA, Sourav NS, Rahman S, Yesmi S, Mia R, Al Noman A, Begum K. Synthesis and investigation of dyeing properties of 8-hydroxyquinoline-based azo dyes. *J Iran Chem Soc.* 2021; 18:817-826. <https://doi.org/10.1007/s13738-020-02070-2>.
8. Fadda A, Abbas N. Synthesis of azo disperse dyes containing pyridine ring for dyeing polyester and polyacrylic fibres. *Pigm Resin Technol.* 2016; 45(1):10–17. <https://doi.org/10.1108/PRT-01-2015-0011>.
9. Arslan O, Aydin B, Yalcin E, Babur B, Seferoglu N, Seferoglu Z. 8-Hydroxyquinoline based push-pull azo dye: novel colorimetric chemosensor for anion detection. *J Mol Struct.* 2017; 1149:499–509. <https://doi.org/10.1016/j.molstruc.2017.08.001>.
10. Ramashetty KB, Channabasappa PM, Seetyanaik BH, Ereshanaik, Ranganai V, Peerya AN, Nayak NH, Shivakumar R, Rajashekarappa KK. Fabrication, depiction, DNA interaction, antibacterial, DFT and molecular docking studies of Co(II) and Cu(II) complexes of 3-methyl-1-phenyl-4-[(E)-(pyridin-2-yl) diazenyl]-1H-pyrazol-5-ol ligand. *Nucl, Nucl Nucleic Acids.* 2021; 41(1):1-22. <https://doi.org/10.1080/15257770.2021.1991373>.
11. Masoud MS, Hemdan SS, Elsamra RMI. Synthesis, ligating properties, thermal behavior, computational and biological studies of some azo-transition metal complexes. *J Inorg Organomet Polym.* 2023; 33:120-137. <https://doi.org/10.1007/s10904-022-02483-x>.
12. Ilina K, Henry M. Cyanine dyes containing quinoline moieties: History, synthesis, optical properties, and applications. *Chemistry.* 2021; 27(13):4230–4248. <https://doi.org/10.1002/chem.202003697>.
13. Ali RR, Mohammed HS. Biological activity and latent fingerprints detection by azo quinoline dye and its complexes. *Period Eng Nat Sci.* 2021; 9(3):317–329. <https://doi.org/10.21533/pen.v9.i3.850>
14. Das A, Lei X. Synthesis and investigation of dyeing properties of 8-hydroxyquinoline based azo dyes and 1-naphthylamine based azo dyes. *J Text Engin Fash Techno.* 2023; 9(6):182-188. <https://doi.org/10.15406/jteft.2023.09.00354>.
15. Geary WJ. The use of conductivity measurements in organic solvents for the characterisation of coordination compounds. *Coord Chem Rev.* 1971; 7(1):81-122. [http://dx.doi.org/10.1016/S0010-8545\(00\)80009-0](http://dx.doi.org/10.1016/S0010-8545(00)80009-0).
16. Abolude IO, Bello KA, Nkeonye PO, Giwa A. Complexation of disperse dyes derived from thiophene with Cu, Co, Zn metal and their application properties on polyester and nylon 6.6 fabrics. *Amer J Sci Engin Techno.* 2021; 6(3):50-63. <https://doi.org/10.11648/j.ajset.20210603.11>.
17. El-Barasi NM, Algazale SF, El-Ajaily MM, Maihub AA, Miloud MM, Al-Noor TH, Mubarak HA, Kareem MM. Synthesis, characterization, theoretical study and biological evaluation of Schiff base and their La (III), Ce(III) and UO₂(II) complexes. *Bull Chem Soc Ethiop.* 2023; 37(2):335-346. <https://dx.doi.org/10.4314/bcse.v37i2.7>.
18. Burca I, Diaconescu AM, Badea V, Péter F. 5-((4-(Phenyldiazenyl)phenyl)diazenyl)quinolin-8-ol. *Molbank.* 2023; 2023(M1701):1-5. <https://doi.org/10.3390/M1701>.
19. Zafar S, Bukhari DA, Rehman A. Azo dyes degradation by microorganisms—An efficient and sustainable approach. *Saudi J Bio Sci.* 2022; 29(12):103437. <https://doi.org/10.1016/j.sjbs.2022.103437>.
20. Hamza IS, Mahmmoud WA, Al-Hamdani AA, Ahmed SD, Allaf AW, Al Zoubi W. Synthesis, characterization, and bioactivity of several metal complexes of (4-amino-(5-methylisaxazol-3-yl)-benzenesulfonamide). *Inorg Chem Comm.* 2022; 144:109776. <http://dx.doi.org/10.1016/j.inoche.2022.109776>.
21. Witwit IN, Mubark HMH, Ali AAM. Synthesis and studying the coordination behavior of a new heterocyclic imidazole azo ligand with some of the first series transition and (IIB) ions. *AIP Conf Proc.* 2020; 2290(1):030025. <https://doi.org/10.1063/5.0027445>.
22. Romerosa A, Saraiba-Bello C, Serrano-Ruiz M, Caneschi A, McKee V, Peruzzini M, Sorace L,

- Zanobini F. Tetrahedral cobalt(II) complexes stabilized by the aminodiphosphine PNP ligand [PNP = CH₃CH₂CH₂N(CH₂CH₂PPh₂)₂]. *Dalt Trans.* 2003; 3(16):3233-3239. <https://doi.org/10.1039/B305443H>.
23. Tetteh S. Coordination behavior of Ni²⁺, Cu²⁺, and Zn²⁺ in tetrahedral 1-methylimidazole complexes: A DFT/CSD study. *Bioinorg Chem Appl.* 2018; 2018:3157969. <https://doi.org/10.1155/2018/3157969>.
 24. Wahba OAG, Hassan AM, Naser AM, Hanafi AM. Preparation and spectroscopic studies of some Copper and Nickel Schiff base complexes and their applications as colouring pigments in protective paints industry. *Egypt J Chem.* 2017; 60(1):25-40. <https://doi.org/10.21608/ejchem.2017.517.1000>.
 25. Nnabuike GG, Salunke-Gawali S, Patil AS, Butcher RJ, Obaleye JA. Synthesis and structures of tetrahedral zinc(II) complexes bearing indomethacin and nitrogen donor ligands. *Inorganica Chimica Acta.* 2020; 513:119941. <https://doi.org/10.1016/j.ica.2020.119941>.
 26. Mahadevi P, Sumathi S. Schiff base metal complexes: Synthesis, optoelectronic, biological studies, fabrication of zinc oxide nanoparticles and its photocatalytic activity. *Res Chem.* 2023; 6:101026. <https://doi.org/10.1016/j.rechem.2023.101026>.
 27. Hussein AO, Al-Khafaji YF, Abbas ZM, Himdan TA. Synthesis, structural characterization, biological evaluation and industrial application of (E)-4-((5-chloro-2-hydroxyphenyl)diazonyl)-1,5-dimethyl-2-phenyl-1H-pyrazol-3(2H)-one and its metal complexes. *Chem Rev Lett.* 2025; 8(3): 460-468. <https://doi.org/10.22034/crl.2024.490959.1480>.
 28. Obaid SMH, Abd-Almonuim AE, Al Naymi HAS, Jarad AJ, Saleh MM. Synthesis and characterization of some metal ions complexes with mixed ligand of azo dye and metformin and evaluation of its effectiveness on the growth of some pathogenic bacteria clinically isolated and study of its toxicity on normal and cancerous hepatocytes. *Heliyon.* 2024; 10(18):e37849. <https://doi.org/10.1016/j.heliyon.2024.e37849>.
 29. Abdulrasool JM. Synthesis, characterization and biological activity of Mn(II), Fe (II), Cd (II), and Hg (II) complexes using (benzo[d]thiazol-2-ylidiazonyl)-4-nitroaniline as novel ligand in the epoxidation of alkenes under thermal and microwave irradiation. *Iran J Cataly.* 2025; 15(1):1-14. <https://doi.org/10.57647/j.ijc.2025.1501.05>.
 30. Al-Adilee KJ, Kyhoiesh HAK, Taher AM. Synthesis, characterization, biological studies, molecular docking and theoretical calculation of some transition metal complexes with new azo dye 2-[2-(6-methoxybenzothiazolyl)azo]-3-methyl-4-nitrophenol. *Res Chem.* 2022; 4(2):100500. <https://doi.org/10.1016/j.rechem.2022.100500>.
 31. Hrichi H, El-Kanzi NA, Ali AM, Abou A. A novel colorimetric chemosensor based on 2-[[[(carbamothioylhydrazono)methyl]phenyl-4-methylbenzenesulfonate (CHMPMPS) for the detection of Cu(II) in aqueous medium. *Res Chem Inter.* 2023; 49(5):1-20. <https://doi.org/10.1007/s11164-022-04905-4>.
 32. Shaalan N. Preparation, spectroscopy, biological activities and thermodynamic studies of new complexes of some metal ions with 2-[5-(2-hydroxy-phenyl)-1,3,4-thiadiazol-2-ylimino]-methyl-naphthalen-1-ol]. *Baghdad Sci J.* 2022; 19(4):829-837. <https://doi.org/10.21123/bsj.2022.19.4.0829>.